INSTITUTE OF PHYSICS PUBLISHING JOURNAL OF MICROMECHANICS AND MICROENGINEERING
J. Micromech. Microeng. **15** (2005) S30–S38 doi:10.1088/0960-1317/15/7/005

Measuring and interpreting the mechanical–thermal noise spectrum in a MEMS

L A Rocha[1], E Cretu[2] and R F Wolffenbuttel[1]

[1] Department for Microelectronics, Faculty of EEMCS, Delft University of Technology, Mekelweg 4, 2628 CD Delft, The Netherlands
[2] Melexis, Transportstr. 1, Tessenderlo, Belgium

Received 26 November 2004, in final form 28 February 2005
Published 20 June 2005
Online at stacks.iop.org/JMM/15/S30

Abstract
The meta-stability of the pull-in displacement of an electrostatically operated parallel plate micromechanical structure is used for the capacitive measurement of the mechanical–thermal noise spectrum in a MEMS. Pull-in time depends on force and is not affected by the input-referred noise of the readout circuit. Repeatedly bringing the microstructure to pull-in while measuring the pull-in time followed by FFT enables the measurement of the mechanical noise spectrum with a non-mechanical noise level set primarily by the resolution of the time measurement. The white noise level is found to be in agreement with the theory on damping. The $1/f$ noise spectrum is found to be independent of ambient gas pressure with a $1/f$ noise–white noise cross-over frequency at 0.007 Hz for a 1 bar gas pressure and is reproducible for devices fabricated in the same process and the same run.

1. Introduction

In a typical mechanical sensor system, electronic circuits are used for readout and processing of the electrical signal provided by the sensing element [1]. The uncertainty (usually total noise level) of the measurement is therefore due to the combined effect of the mechanical–thermal noise in the mechanical domain [2], the electrical noise of the (resistive) mechanical sensing element and the input referred noise of the readout circuits. Direct measurement of the mechanical–thermal noise (i.e. not significantly affected by the circuit noise) is possible in the case of a transduction effect of extremely good resolution, since the mechanical input referred values of the circuit noise are proportionally reduced, or in the case of a high mechanical–thermal noise level. Electron tunnelling transducers offer a displacement resolution approaching 10^{-14} m Hz$^{-1/2}$, which is sufficient for the circuit noise to be disregarded in a properly designed MEMS (microelectromechanical system) for inertial sensing [3]. Microphones require a relatively large membrane for acoustic interaction, which results in a relative large damping and hence in a relatively large noise level. The membrane mechanical–thermal noise can be directly measured using a high-performance capacitive or electret microphone [4, 5]. However, in a typical MEMS readout circuit noise dominates the noise performance [6]. As a consequence the details of the mechanical–thermal noise are often not considered relevant, and the electronic noise determines the detection limit of the sensor. More fundamental studies on noise and damping are hampered by the same fact, as the mechanical–thermal noise cannot be directly measured. An estimation of the mechanical–thermal noise can be made from the total sensor noise by a careful analysis or selective measurement of the electrical noise [7].

In this paper the meta-stability of the pull-in displacement of an electrostatically operated parallel-plate structure [8] is used for the capacitive measurement of mechanical–thermal noise spectrum. The use of the pull-in time as a sensing mechanism removes circuit noise as a limiting factor in mechanical noise analysis, since pull-in time depends on force and is not affected by the input referred noise of the readout circuit. The total noise level is in this case due to the mechanical–thermal noise of the structure and the non-mechanical noise set by the resolution of the time measurement. Repeatedly bringing the microstructure to pull-in while measuring the pull-in time followed by FFT enables the measurement of the mechanical noise spectrum with a non-mechanical noise set primarily by the resolution of the

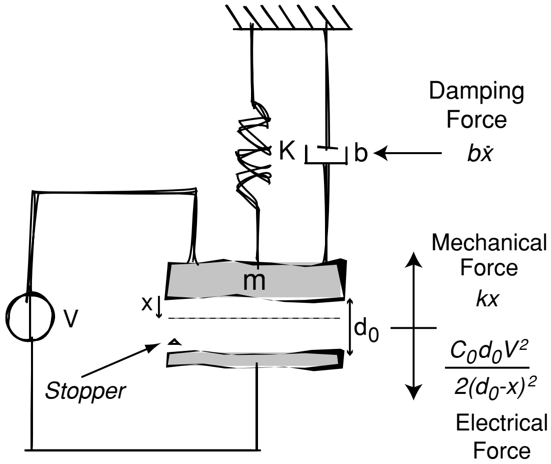

Figure 1. MEMS device schematic.

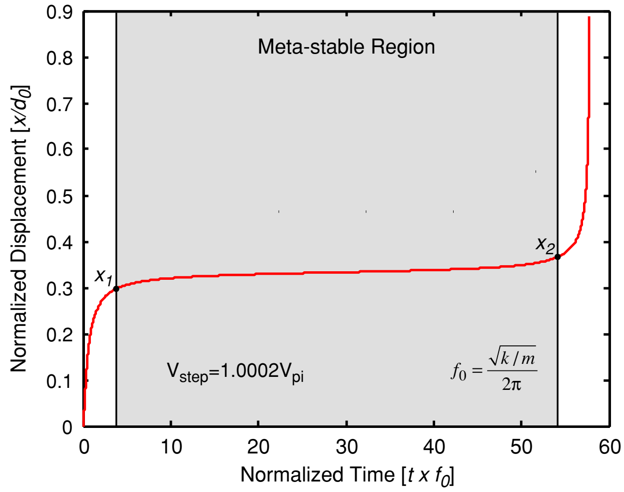

Figure 2. Pull-in displacement characteristic: meta-stable region.

time measurement. The white noise level is found to be in agreement with the theory on damping. Moreover, long-term measurements have provided essential information for the investigation of $1/f$ mechanical noise in low-Q MEMS.

2. Dynamic pull-in: meta-stable region

The simplified prototype of a parallel-plate microelectromechanical device is presented in figure 1. Four lumped elements can be used for a physical modelling of the device: a movable parallel-plate capacitor actuated by a supply voltage, the mass of the movable structure, an elastic spring (suspension system) and a damper. In the case of an external acceleration, a_{ext}, the equilibrium of forces is written as

$$m\frac{\mathrm{d}^2x}{\mathrm{d}t^2} + b\left(x, \frac{\mathrm{d}x}{\mathrm{d}t}\right)\frac{\mathrm{d}x}{\mathrm{d}t} + kx = ma_{\text{ext}} + F_{\text{elect}}, \tag{1}$$

where x is the structure displacement, m represents the movable mass, b is the (nonlinear) damping coefficient, k is the spring constant and $F_{\text{elect}} = \frac{C_0 d_0 V^2}{2(d_0-x)^2}$ is the electrostatic force caused by a voltage V applied to a capacitor with initial value C_0 and initial gap d_0. If the device is overdamped and a step voltage, V_{step}, slightly higher than the static pull-in voltage, $V_{\text{pi}} = \sqrt{\frac{8}{27}}d_0\sqrt{\frac{k}{C_0}}$ [9], is applied to the structure ($V_{\text{step}} = \alpha V_{\text{pi}}$, with $1 < \alpha < 1.1$), a pull-in motion characterized by a meta-stable region is observed (figure 2).

The time spent in the meta-stable region is very sensitive to any external force and thus this time is a measure of any external force. Since the meta-stable region is characterized by a tight equilibrium between elastic and electrostatic forces at a very well defined displacement ($x_{\text{pi}} = d_0/3$), it suggests that a small signal analysis around the pull-in displacement is enough for a mathematical description of this region. A linear second-order system results using a local linearization of (1) around x_{pi}. Expressing the change in position, $x - x_{\text{pi}}$, as variable y, while assuming $V = \alpha V_{\text{pi}}$, the linearized expression of y during the meta-stable regime in the Laplace domain results:

$$Y(s) = \frac{a_{\text{ext}}(s) + \frac{kd_0}{3m}(\alpha^2 - 1)}{s^2 + \frac{b}{m}s + \frac{k}{m}(1-\alpha^2)}. \tag{2}$$

For a positive value of α, the linearized Laplace expression presents two poles, a positive and a negative. The positive pole is the dominant one and is the cause for the system instability. The negative pole can therefore be neglected, without introducing large errors, obtaining a simplified Laplace expression. The time, t_m, necessary to go from an initial position, x_1 (start of the meta-stable region, figure 2) to a final position, x_2 (end of the meta-stability, figure 2) is obtained by making the inverse Laplace of the simplified expression and by solving the resultant system in variable t, considering a displacement $\Delta x = x_2 - x_1$ [10]:

$$t_m = \frac{\ln\left[\frac{(k(\alpha^2-1)(d_0+3\Delta x)+3ma_{\text{ext}})^2}{(d_0k(\alpha^2-1)+3ma_{\text{ext}})^2}\right]\left(b + \sqrt{4km(\alpha^2-1)+b^2}\right)}{4k(\alpha-1)(\alpha+1)}. \tag{3}$$

By exploiting this sensitive region in the absence of an external force, the equivalent noise force can be measured and compared to theory on mechanical–thermal noise. The fabricated structure and experimental setup used for this purpose are explained in detail in the next two sections.

3. Noise analysis

The thermally excited random vibration of charge carriers that is the origin of white noise in an electrical resistor is also applicable to gas damping. The random movement of the molecules in gas at a certain temperature and surrounding the mechanical structure leads to random fluctuations in the energy transfer between structure and damping gas, which is generally referred to as mechanical–thermal noise [2, 11]. According to [2], any mechanical system in thermal equilibrium, no matter how complex, can be analysed for mechanical–thermal noise by adding a force generator alongside each damper. For the parallel-plate MEMS device, the general equation of motion, considering a constant damping coefficient, becomes

$$m\frac{\mathrm{d}^2x}{\mathrm{d}t^2} + b\frac{\mathrm{d}x}{\mathrm{d}t} + kx = ma_{\text{ext}} + F_{\text{elect}} + F_{\text{noise},b}, \tag{4}$$

where $F_{\text{noise},b}$ represents the random contribution of the different noise generating processes. Because a thermal equilibrium between the MEMS device and the surroundings is assumed, the energy lost towards the environment through the dissipative friction (damping coefficient) must equal on

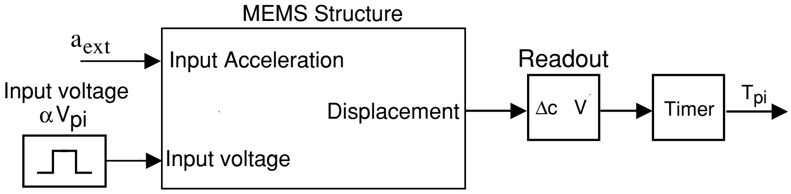

Figure 3. Pull-in time measuring setup.

average the energy gained through the noise force. Nyquist's theorem [2] relates the noise force spectral density to mechanical resistance (damping coefficient):

$$F_{\mathrm{noise},b}(f) = \sqrt{4k_{\mathrm{B}}Tb}\ [\mathrm{N}/\sqrt{\mathrm{Hz}}], \tag{5}$$

where k_{B} is the Boltzmann constant (1.38×10^{-23} J K^{-1}) and T is the absolute temperature. The theorem remains valid in the case of a non-linear and frequency dependent damping, which is the case in a typical MEMS [8]. The mechanical–thermal force noise of the microstructure is therefore governed by the Nyquist theorem. As mentioned in the introduction, direct experimental verification of the mechanical–thermal noise in a MEMS operating in the linear displacement regime is hampered by the equivalent input noise power of the readout. However, using the highly non-linear pull-in mode offers a technique for noise sampling not affected by the readout circuits and can be used for mechanical–thermal noise analysis, as is shown in the next section.

3.1. Setup noise analysis

The full setup for noise measurement is depicted in figure 3. A square-wave signal with amplitude αV_{pi} is applied to the MEMS device. The displacement is measured by sensing the changes in capacitance. The readout circuit transforms the changes in capacitance, ΔC, into a voltage V, and the pull-in time is measured using a timer with a resolution Δt, i.e. two threshold values are set and continuously compared with the capacitively measured position to start and stop the time clock. The essential sub-systems in this measurement setup are the power supply, the microstructure, the readout circuit and the timer. Variations in pull-in time may result from any of these sub-systems, whereas the purpose is to analyse the microsystem mechanical–thermal noise spectrum. Therefore, these subsystems need to be investigated to verify whether they significantly affect the uncertainty in the pull-in time measurement.

1. *Power supply*. Pull-in time depends strongly on the voltage applied. Moreover, this voltage needs to be tuned very precisely to a value slightly higher than V_{pi}. High stability is essential and thus the effect needs to be experimentally verified.
2. *MEMS device*. The mechanical structure is expected to be the main noise source of the system. Due to the high-sensitivity of the meta-stable region, the time-output is a measure for the noise force. A convenient property of pull-in time measurements is the time averaging of high-frequency components in the noise force, which consequently do not contribute to variations in the displacement. Only frequencies lower than $2/t_{\mathrm{pi}}$ are present during the full pull-in movement [12]. This property limits the noise spectral frequency range measured. This is not a problem since the interesting features are in the low frequency part. The total noise force is therefore
$$F_{\mathrm{noise},b} = \sqrt{\frac{8k_{\mathrm{B}}Tb}{t_{\mathrm{pi}}}}[\mathrm{N}] \tag{6}$$
3. *Front-end electronics*. The function of the readout circuits is to provide sufficient gain for the pull-in time to serve as a gating signal in a counter. A charge amplifier is used for this purpose with equivalent input noise sources specified. The influence of the equivalent input noise can be reduced to a negligible level, by a proper setting of the trigger window.
4. *Timer*. A data acquisition board (DAQ) is responsible for the acquisition of the voltage equivalent displacement and for measuring pull-in time. The sampling frequency, f_{s}, introduces uncertainty in the measured pull-in time in the form of quantization noise.

The dependence of the pull-in voltage on device structure and external parameters also needs to be taken into account for a rigorous analysis of the mechanical–thermal noise. The pull-in voltage depends on both the mechanical properties of the material [13] and any residual stress. However, these effects can be limited by a careful design, and high-stability has been achieved [14, 15]. Long-term measurements presented in [16] report on a charging effect during the first hours of operation and a temperature dependence due to thermal expansion of the material and temperature dependence of Young's modulus. Since the changes in ambient temperature are relatively slow, they are not expected to affect the white noise level, however, they should be considered in a long-term noise analysis ($1/f$ noise). The charge dependence of the pull-in voltage is circumvented using a burn-in period prior to performing measurements [16].

4. Experimental results and analysis

The microstructure shown in figure 4, fabricated in the Bosch epi-poly process [17, 18], was used for the experimental measurements of the dynamic pull-in transition. The device has four folded beams, 340 μm long and 2.5 μm wide, connected to two rigid central bars of about 1 mm length. Parallel-plate capacitors with a 2.25 μm gap are used for the actuation of the movable mass. The nominal (designed) gap is 2 μm. The actual values have been derived from SEM photographs as in figure 4. The displacement measurement involves sensing the changes of various sets of differential capacitors. Stoppers, located on the end of the rigid bars, 2 μm apart, prevent the electrodes from touching after pull-in is reached. The main device characteristics are presented in table 1.

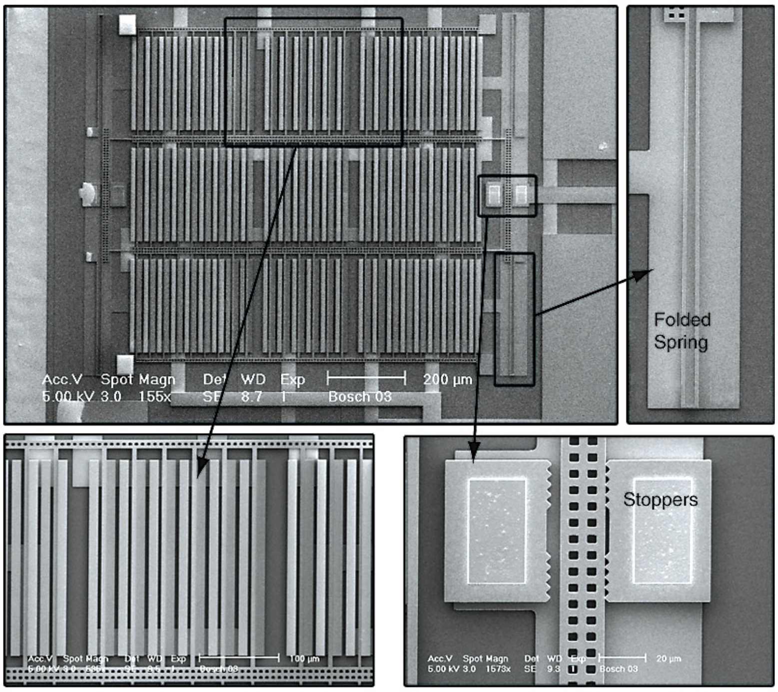

Figure 4. Fabricated MEMS device.

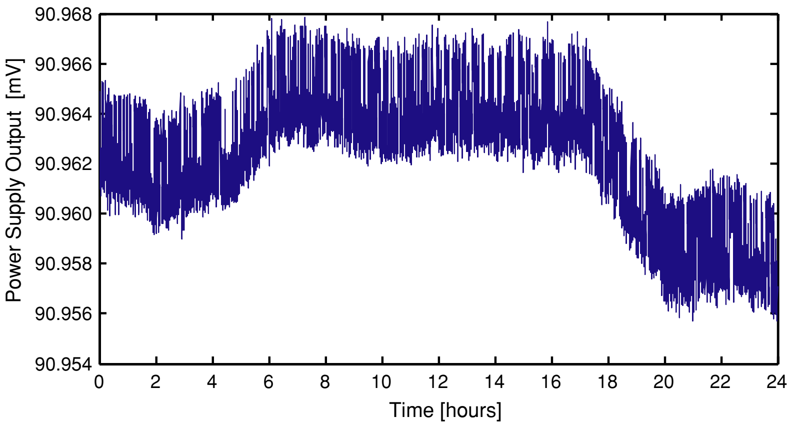

Figure 5. Power supply noise measured at 28 °C ± 1 °C.

Table 1. Main parameters of the microstructure (computed from the photograph of the actual device and bulk material values).

Parameter	Value
Mass (m)	4.27 μg
Mechanical spring (k)	1.2930 N m^{-1}
Initial gap (d_0)	2.25 μm
Damping coefficient (b) (linearized around $x = d_0/3$) [8]	1.92×10^{-4} Ns m^{-1}
C_{d0} (zero-displacement actuation capacitor)	141 fF
C_{s0} (zero-displacement sensing capacitor)	611 fF
Pull-in voltage (V_{pi})	3.708 V

4.1. Measurement setup

The specifications of the individual blocks implemented in the system in figure 3 must be sufficient to ensure that the total system noise is set by the mechanical–thermal noise of the MEMS structure. The power supply used (Yokogawa 7651) has a stability specified to be better than 20 μV d^{-1} and a noise level at 16 μV for a 10 kHz bandwidth. Since these noise specifications are incomplete (no $1/f$ noise mentioned) the power supply was sampled with a frequency of 0.5 Hz by a 1 μV resolution multimeter and the results are shown in figure 5. These measurements confirm both the power supply stability and the low noise levels, and therefore the power supply noise can be neglected as compared to the mechanical–thermal noise of the MEMS device.

A single-ended output circuit [19] has been used to measure the displacement of the fabricated MEMS device. The capacitance is measured by driving both terminals of the capacitive bridge and taking the centre node as the output terminal (common to both capacitors). A schematic of the realized circuit for differential capacitive displacement detection is depicted in figure 6. The core of the circuit is the charge amplifier.

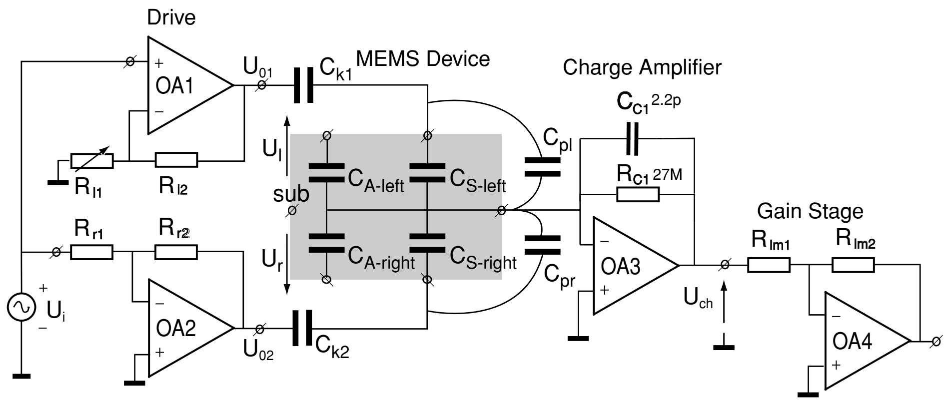

Figure 6. Displacement detection circuit.

A carrier signal, U_i, is applied to the drive amplifiers resulting in two voltages in opposite phase, U_{01} and U_{02}, which drive the differential capacitive pair $C_{\text{s-left}}$ and $C_{\text{s-right}}$. C_{k1} and C_{k2} are large coupling capacitors (0.1 μF) to prevent any dc signal coupling to the sensing electrodes. When a carrier voltage is applied to the sensing capacitors, the transfer function of the MEMS device to the charge-amplifier is expressed by

$$U_{\text{ch}} = \left(\frac{C_{\text{s-left}} + C_{\text{pl}}}{C_{c1}}\right) U_l - \left(\frac{C_{\text{s-right}} + C_{\text{pr}}}{C_{c1}}\right) U_r, \qquad (7)$$

where C_{pl} and C_{pr} are parasitic capacitances. These parasitic capacitances are due to the housing and bondpad connections. Since the parasitic capacitances have a much higher value as compared to the MEMS sensing capacitances, these could give rise to a large signal offset at the charge amplifier. U_{01} is made adjustable (using R_{l1}) and is used to compensate the offset of the charge amplifier at the expense of a nonlinear gain setting due to the different amplitudes of U_{01} and U_{02}. Consequently, the amplitude of the carrier signal, U_i, is modulated by the capacitance changes and is available at the output of the gain stage.

The single-ended readout circuit was implemented at the PCB level. For the driving amplifiers, OA_1 and OA_2, two AD8041 operational amplifiers were used, whereas the charge amplifier, OA_3, and the gain stage amplifier, OA_4, were implemented using the LF356 operational amplifiers. This results in a measured output white noise level at 188 nV Hz$^{-1/2}$. A lock-in amplifier is used (SR830 from Stanford Research Systems) for demodulation of the output signal. The noise bandwidth is 4.8 kHz (set by a fourth-order low-pass filter implemented after the demodulator), which results in a total noise of the readout circuit of about 13 mV. The sampling frequency of the DAQ is at 100 kHz, resulting in an uncertainty in the measured pull-in time of 10 μs, which is basically the quantization noise of the DAQ. The slew rate at the onset and final phase of the pull-in transition is of sufficiently high value to allow the circuit equivalent input noise to be disregarded. As shown in figure 7, the rate of change of displacement versus time exceeds 10 mV μs^{-1}, which allows for the selection of trigger levels in such a way that the uncertainty due to readout circuit noise is smaller than the quantization noise of the 10 μs sampling.

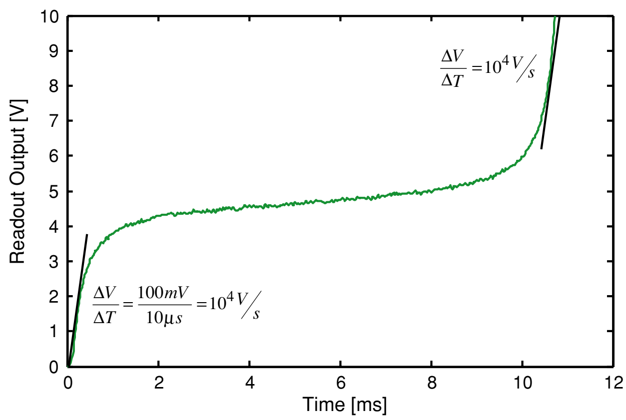

Figure 7. Measurement of a typical pull-in dynamic transition.

4.2. Measurement results

Measurements were performed on one fabricated device with air at atmospheric pressure (1 bar) as the surrounding gas medium for the duration of one day. A square-wave input voltage with 5 Hz and amplitude $\alpha = 1.0008$ was used. The measuring setup was introduced in a climate chamber at a temperature of 30 ± 0.5 °C. Care was taken to minimize the effect of external accelerations. The device was placed in a plane perpendicular to the gravitational field and, therefore, the only source of uncertainty results from random vibrations of the building. These are estimated to be much smaller then the microstructure white noise level and are disregarded. The time series of the measured pull-in times is presented in figure 8.

Since the sensitivity of the sensor to external accelerations can be computed using (2), the measured time-changes can be directly translated to the momentary value of the equivalent force. In the absence of any time-varying external acceleration, this force is due to the momentary value of the mechanical–thermal noise. From figure 2 and table 1 follows: $\Delta x = 0.05$ μm and the sensitivity results as $S = 0.016$ s m^{-1} s^{-2} for $\alpha = 1.0008$. This value for S is confirmed by more complex modelling that does not rely on the simplifications introduced in the derivation of equation (2) [8, 20]. The average value of the pull-in time is $t_{\text{pi,mean}} = 12$ ms and the standard deviation (noise value) is $\sigma_{\text{pi}} = 112$ μs (for 500 samples). The equivalent noise acceleration can be

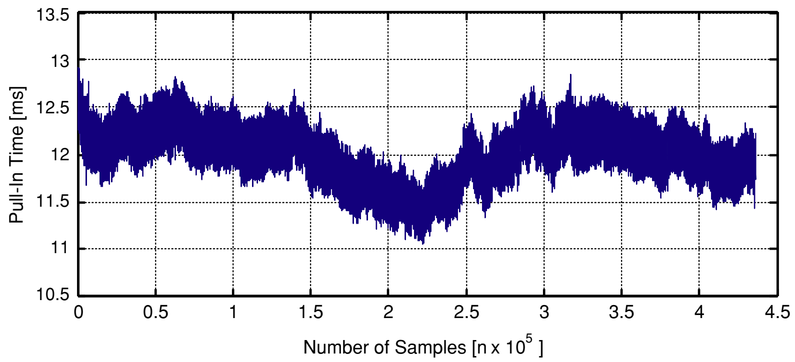

Figure 8. The time series of measured pull-in time at 1 bar and $\alpha = 1.0008$.

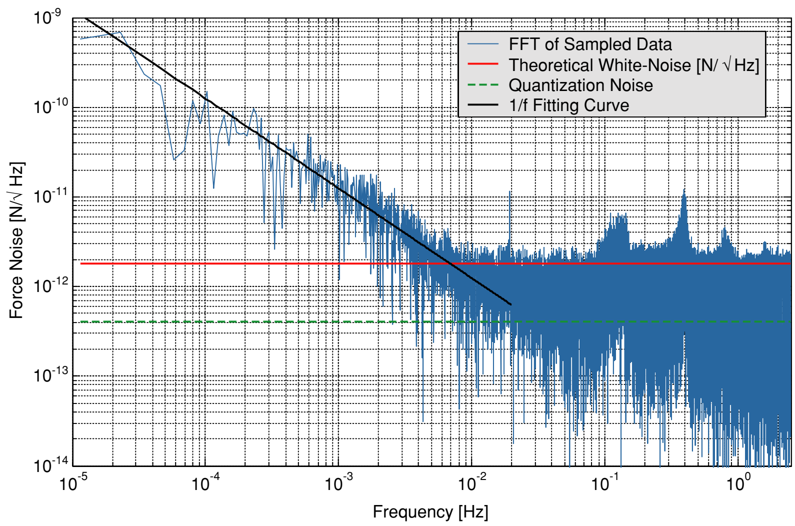

Figure 9. FFT of the sampled pull-in time at 1 bar and $\alpha = 1.0008$.

calculated as $a_n = \sigma_{\text{pi}}\ S^{-1} = 7 \times 10^{-3}$ m s^{-2} and the total measured noise force becomes $F_n = ma_n = 2.98 \times 10^{-11}$ N. Equation (5) can be used for computing the total noise force to verify this experimental result. A complication results from the damping coefficient, which, amongst others, depends on the momentary gap width during pull-in motion and thus is not constant during the pull-in event. However, the movable electrode spends most of its time around the static pull-in displacement (meta-stable region), which justifies the use of a constant damping coefficient calculated at $x_{\text{pi}} = (1/3)d_0$. The value of the damping coefficient is shown in table 1 for air at atmospheric pressure as the gas medium. For a pull-in time of 12 ms, the predicted equivalent input total noise force given by equation (5) is: $F_{\text{noise}} = 2.3 \times 10^{-11}$ N. The sensitivity S can also be used to evaluate the significance of the noise sources introduced by the other system components. The 10 μs uncertainty of the DAQ can be converted to a noise force and the total predicted white noise level increases to $(10 \times 10^{-6}\ \text{m})\ S^{-1} + 2.3 \times 10^{-11} = 2.56 \times 10^{-11}$ N, which is in good agreement with the measured value. These measurements confirm the noise analysis made to the pull-in measuring system and clearly show that the mechanical–thermal noise can be measured.

More interesting conclusions can be made after taking the FFT of the measured data. The result of a FFT on the series of pull-in time measurements in figure 8 is shown in figure 9. The curve is calibrated in terms of noise spectral density by correcting for bandwidth. The most significant properties are the agreement with the theoretical mechanical–thermal white noise spectral density and the increasing noise spectral density with decreasing frequency. The latter observation strongly suggests the presence of the $1/f$ noise in the micromechanical domain. Since $1/f$ noise is demonstrated in all physical domains, this is not unexpected. The $1/f$ noise–white noise cross-over frequency is at the surprisingly low value of 0.007 Hz, especially when considering recent reports on microphone $1/f$ noise [5]. Consequently, some caution seems appropriate before claiming that this is indeed the $1/f$ noise originating from the MEMS and additional experiments were performed.

4.3. $1/f$ noise

The so-called $1/f$ noise is characterized by a noise spectral power $P(f) = 1/f^a$, where the exponent a is very close to 1 [21, 22]. There is no generally accepted explanation for the $1/f$ noise and the theories used to explain the phenomenon are usually only valid under very specific conditions and in a specific physical domain. For this reason $1/f$ noise is not well

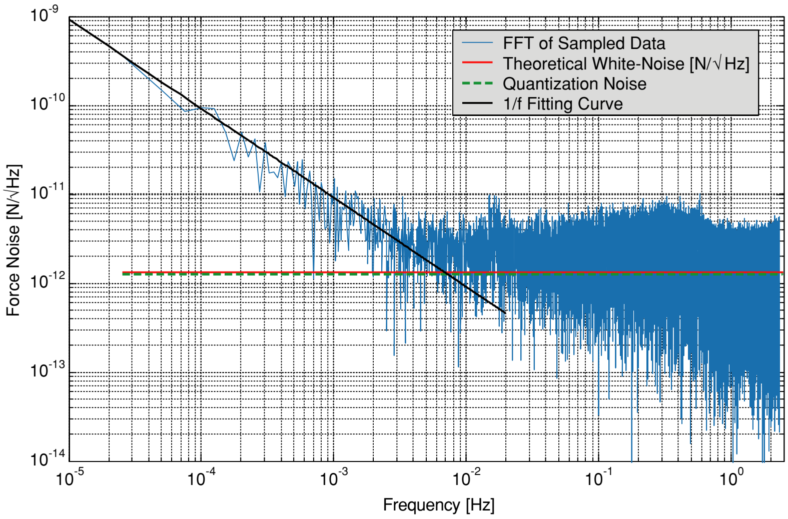

Figure 10. FFT of measured samples at 200 mbar and $\alpha = 1.002$.

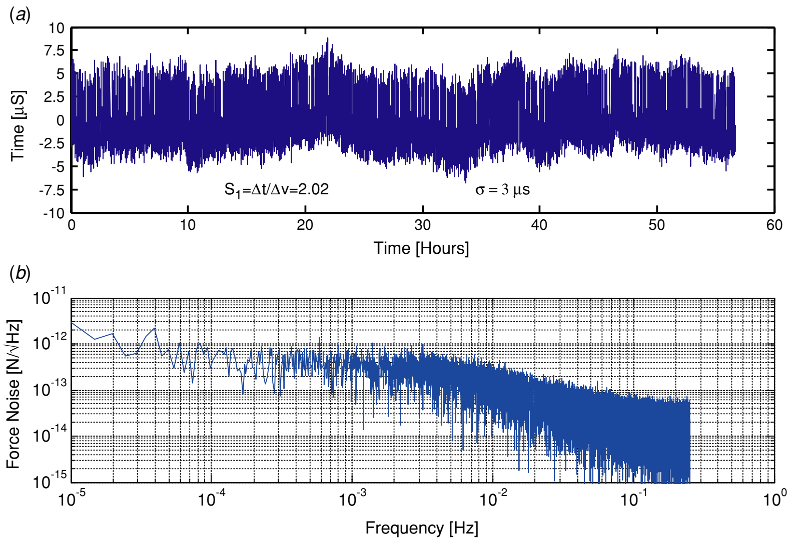

Figure 11. Sampling of the power supply at constant temperature. (*a*) Time series and (*b*) FFT.

understood. This state-of-the-art is not helpful in interpreting figure 9.

Additional measurements were therefore performed for supporting the claim that the $1/f$ noise originates from the mechanical structure. The FFT of the time series of the pull-in time measurements at a pressure of 200 mbar ($\alpha = 1.002$) is presented in figure 10. Theory on mechanical–thermal white noise predicts a noise spectral power proportional to damping and thus a noise per square root of hertz reducing with pressure. However, pull-in time also reduces with pressure and therefore sensitivity decreases. For short pull-in times and low sensitivities the quantization noise tends to be the dominant noise source. For the particular case of the 200 mbar measurements the quantization noise is in the same order of magnitude as the predicted white noise per square root of hertz and consequently the measured white noise per square root of hertz has an higher value as compared to the previous 1 bar measurement. These considerations are all confirmed by the data in figure 10. Moreover, and most significantly, the asymptotic best fit for the $1/f$ noise does not shift over the spectrum, which suggests that the measured $1/f$ noise indeed originates from the mechanical structure and is independent of air damping.

Additional data are needed to conclusively dismiss the power supply as the source of the $1/f$ noise. The power source was again sampled at constant temperature, but this time for 50 h (figure 11(*a*) with a 1 μV resolution and a sampling frequency of 0.5 Hz. Using (2), the sensitivity of the pull-in time with respect to the applied voltage can be computed. A value of $S_1 = \Delta t/\Delta V = 2.02$ for $\Delta x = 0.05$ μm and $\alpha = 1.0008$ is found. The time noise due to the voltage noise can then be translated to a total noise force $F_n = \frac{(\sigma \times S_1)m}{S} = 16.10^{-13}$ N, which is almost a factor 20 smaller than the measured force noise of the MEMS, $F_n = ma_n = 2.98 \times 10^{-11}$ N (assuming the same operation conditions apply). The FFT of the sampled data is shown in figure 11(*b*). The data are expressed in terms of equivalent force noise and directly comparable with the data of figure 9

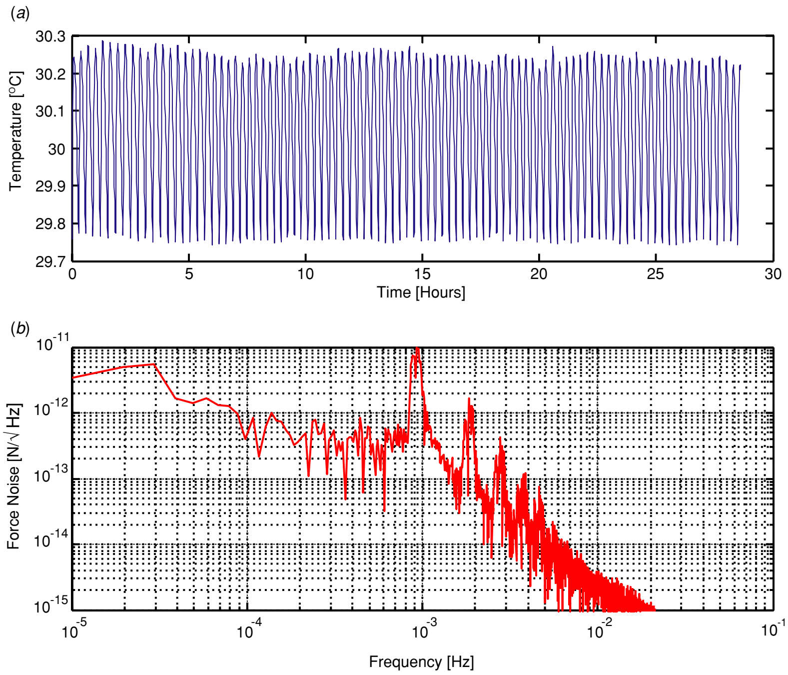

Figure 12. Measured temperature inside the oven. (*a*) Time series and (*b*) FFT.

(noise force). The noise force caused by the power supply is indeed very small and can be neglected, which implies that the origin of the $1/f$ is not the power supply.

Another source of uncertainty mentioned in section 3.1 is the stability of the pull-in voltage, V_{pi}. The pull-in study performed in [16] reveals a charge effect and a temperature dependence of the pull-in voltage. To eliminate the charge effect, burn-in periods were performed before the noise measurements. Finally, temperature effects should be considered. The temperature coefficient of the pull-in voltage is described by [16]

$$\frac{\partial V_{pi}}{\partial T} = V_{pi}\frac{\gamma+\beta}{2\sqrt{(1+(\gamma+\beta)T)}}, \tag{8}$$

where γ and β are the polysilicon thermal expansion coefficient and Young's modulus thermal coefficient respectively. For $\gamma = 3\times10^{-6}\,\mathrm{K}^{-1}$ and $\beta = -67\times10^{-6}\,\mathrm{K}^{-1}$ [23] the expected pull-in voltage temperature coefficient is $-118\ \mu$V. The temperature oscillations inside the oven have been recorded and are presented in figure 12(*a*). The oscillations are within 0.5 °C reducing the pull-in voltage uncertainty to 59 μV. The thermal time constant of the packaged microstructure has been characterized by experiment and can be described by a first-order thermal filter with a cut-off frequency at 10^{-3} Hz. This thermal filter implies that fast temperature variations are averaged by the package thermal behaviour. This reduces any concerns about the effect on the white level noise, but does not *a priori* rule out any effect on the $1/f$ spectral range. Applying this low-pass filter with unit gain in the passband to the data of figure 12(*a*) and subsequently converting the temperature oscillations to an equivalent noise force (similar to the power supply $1/f$ noise calculation), the graph of figure 12(*b*) results. The FFT shows a flat line at low frequencies below the measured $1/f$ level. Therefore, the temperature oscillations are not the cause for the measured $1/f$ noise. Nevertheless, the high sensitivity of the pull-in voltage to temperature oscillations implies that the temperature needs to be kept stable and well characterized for a meaningful study of the noise mechanisms using the high-sensitive meta-stable region.

5. Conclusions

This paper presents an analysis and measurements of the noise mechanisms in MEMS. The mechanical–thermal white noise has been measured. The results are reproducible for devices fabricated in the same process and the same run and show a spectral density depending on the pressure of the surrounding damping air. The $1/f$ noise spectral density is found to be independent of ambient gas pressure and reproducible for devices fabricated in the same process and the same run. The $1/f$ noise-mechanical–thermal white noise cross-over frequency is at 0.007 Hz in the case of air at 1 bar surrounding the microstructure.

The advantage of the high sensitivity of the meta-stable region has been demonstrated and has yielded a very useful tool to study fundamental MEMS noise mechanisms. The mechanical–thermal white noise measured is in agreement with existing theory on damping and mechanical–thermal noise. The measurements are not conclusive with respect to the identification of the MEMS as the source of the $1/f$ noise, however they lead to a sufficient level of confidence to draw preliminary conclusions. More extensive analysis is needed to fully validate the results presented here. In general $1/f$ noise is known to be, amongst others, defect related and could, therefore, in the micromechanical domain be due to the surface roughness of the moving surfaces. The data-acquisition used limits the frequency range to 2.5 Hz and yields a high level of quantization noise. An improved performance data-acquisition system and measurement results on a range of microstructures of different design and surface roughness are required to actually identify and explain the origins of $1/f$ noise in MEMS.

References

[1] Wolffenbuttel R F 1996 *Silicon Sensors and Circuits; On-Chip Compability* (London: Chapman and Hall)

[2] Gabrielson T B 1993 Mechanical–thermal noise in micromachined acoustic and vibration sensors *IEEE Trans. Electron Devices* **40** 903–9

[3] Rockstad H K, Kenny T W, Reynolds J K, Kaiser W J and Gabrielson A T B 1994 Miniature high-sensitivity broad-band accelerometer based on electron tunneling transducers *Sensors Actuators* **A 43** 107–114

[4] Zuckerwar A J 1994 Measured $1/f$ noise in the membrane motion of condenser microphones *J. Acoust. Soc. Am.* **95** 1419–25

[5] Zuckerwar A J and Kuhn T R 2003 Background noise in piezoresistive, electret condender and ceramic microphones *J. Acoust. Soc. Am.* **113** 3179–87

[6] Amini B V, Pourkamali S and Ayazi F 2004 A high resolution, stictionless, CMOS compatible SOI accelerometer with a low noise, low power, 0.25 μm CMOS interface *Proc. MEMS'04 (Maastricht, The Netherlands, 25–29 January 2004)* pp 572–5

[7] Chae J, Kulah H and Najafi K 2003 A monolithic three-axis silicon capacitive accelerometer with micro-G resolution *Proc. Transducers'03 (Boston, MA, 8–12 June 2003)* pp 81–4

[8] Rocha L A, Cretu E and Wolffenbuttel R F 2004 Behavioural analysis of the pull-in dynamic transition *J. Micromech. Microeng.* **14** S37–S42

[9] Tilmans H A C and Legtenberg R 1994 Electrostatically driven vacuum-encapsulated polysilicon resonators: part 2. Theory and performance *Sensors Actuators* A **45** 67–84

[10] Rocha L A, Cretu E and Wolffenbuttel R F 2004 Analytical model for the pull-in time of low-Q MEMS devices *Proc. Nanotech 2004 (Boston, MA, 7–11 March 2004)* pp 271–4

[11] Djuric Z 2000 Mechanisms of noise sources in microelectromechanical systems *Microelectron. Reliab.* **40** 919–32

[12] Rocha L A, Cretu E and Wolffenbuttel R F 2004 Pull-in dynamics: analysis and modeling of the transitional regime *Proc. MEMS'04 (Maastricht, The Netherlands, 25–29 January 2004)* pp 249–52

[13] Peterson K E 1982 Silicon as a mechanical material *Proc. IEEE* **70** 420–57

[14] Oja A S, Kyynäräinen J, Seppä H and Lampola T 2000 A micromechanical dc voltage reference *Conf. Digest. CPEM'00 (Sydney, Australia, 14–19 May 2000)* pp 701–2

[15] Cretu E, Rocha L A and Wolffenbuttel R F 2001 Micromechanical voltage reference using the pull-in of a beam *IEEE Trans. Instrum. Meas.* **50** 1504–7

[16] Rocha L A, Cretu E and Wolffenbuttel R F 2004 Compensation of temperature effects on the pull-in voltage of microstructures *Sensors Actuators* A **115** 351–6

[17] http://www.europractice.bosch.com/en/start/index.htm

[18] Offenberg M, Lärmer F, Elsner B, Münzel H and Riethmüller W 1995 Novel process for an integrated accelerometer *Proc. Transducers95 (Stockholm, Sweden, 25–29 June 1995)* pp 589–93

[19] Burstein A and Kaiser W J 1995 Mixed analog–digital highly-sensitive sensor interface circuit for low-cost microsensors *Proc. Tranducers95 (Stockholm, Sweden, 25–29 June 1995)* pp 162–5

[20] Rocha L A, Cretu E and Wolffenbuttel R F 2003 Displacement model for dynamic pull-in analysis and application in large-stroke electrostatic actuators *17th Proc. Eurosensors (Guimarães, Portugal) 2003* pp. 448–51

[21] West B J and Schlesigner M F 1990 The noise in natural phenomena *Am. Sci.* **78** 40–45

[22] Wong H 2003 Low-frequency noise study in electron devices: review and update *Microelectron. Reliab.* **43** 585–99

[23] Bosch 2002 *Micromachining Foundry Design Rules* version 3.0